metals

MDPI

Article

Metal Posts and the Effect of Material–Shape Combination on the Mechanical Behavior of Endodontically Treated Anterior Teeth

Antonio Gloria [1,*], Saverio Maietta [2,*], Maria Richetta [3], Pietro Ausiello [4] and Massimo Martorelli [2]

1 Institute of Polymers, Composites and Biomaterials, National Research Council of Italy, V.le J.F. Kennedy 54-Mostra d'Oltremare Pad. 20, 80125 Naples, Italy
2 Department of Industrial Engineering, Fraunhofer JL IDEAS, University of Naples Federico II, P.le Tecchio 80, 80125 Naples, Italy; massimo.martorelli@unina.it
3 Department of Industrial Engineering, University of Rome Tor Vergata, 00133 Rome, Italy; richetta@uniroma2.it
4 School of Dentistry, University of Naples Federico II, via S. Pansini 5, 80131 Naples, Italy; pietausi@unina.it
* Correspondence: angloria@unina.it (A.G.); smaietta@unina.it (S.M.); Tel.: +39-081-242-5942 (A.G. & S.M.)

Received: 16 December 2018; Accepted: 22 January 2019; Published: 24 January 2019



Abstract: The control of the process–structure–property relationship of a material plays an important role in the design of biomedical metal devices featuring desired properties. In the field of endodontics, several post-core systems have been considered, which include a wide range of industrially developed posts. Endodontists generally use posts characterized by different materials, sizes, and shapes. Computer-aided design (CAD) and finite element (FE) analysis were taken into account to provide further insight into the effect of the material–shape combination of metal posts on the mechanical behavior of endodontically treated anterior teeth. In particular, theoretical designs of metal posts with two different shapes (conical-tapered and conical-cylindrical) and consisting of materials with Young's moduli of 110 GPa and 200 GPa were proposed. A load of 100 N was applied on the palatal surface of the crown at 45° to the longitudinal axis of the tooth. Linear static analyses were performed with a non-failure condition. The results suggested the possibility to tailor the stress distribution along the metal posts and at the interface between the post and the surrounding structures, benefiting from an appropriate combination of a CAD-based approach and material selection. The obtained results could help to design metal posts that minimize stress concentrations.

Keywords: dental materials; metal posts; computer-aided design (CAD); image analysis; mechanical properties; finite element analysis

1. Introduction

The development of biomedical metal devices featuring desired properties always requires control of the process–structure–property relationship for a material. Thus, from a material point of view, process parameters are important to obtain a suitable microstructure and, hence, specific properties, whereas the material–shape combination represents a further feature which allows the design of devices with improved and tailored properties.

With regard to industrial metal manufacturing, the relationship among process parameters, microstructure, and mechanical properties is of great interest in different areas (e.g., casting, plastic forming, sintering, and welding), and also involves traditional and innovative processes [1–3].

In the field of endodontics, the fracture resistance of teeth should be improved by cementing a post into the root [4,5]. Generally, cast metal posts and prefabricated posts are employed. The use

of cast metal posts requires expensive and time-consuming procedures as well as a direct pattern or impression of the root cavity, whereas prefabricated posts involve less expensive and straightforward procedures which can be carried out in a single visit [4].

Prefabricated posts are usually characterized by parallel or tapered forms and are made of anisotropic materials (e.g., fiber-reinforced composite—FRC) or isotropic materials (e.g., gold alloy, titanium, and nickel-chromium alloy) [5–8].

The levels of stress and strain generated in endodontically treated teeth are strongly related to the employed post-and-core systems [4]. Nevertheless, it remains unclear whether a flexible or stiff post is needed. The risk of root fracture in endodontically treated teeth depends upon the restoration stiffness, and many studies focusing on which material might reduce stresses suggest that neither flexible nor stiff posts are ideal [4,5]. Cast posts and prefabricated metal posts usually generate high stresses at the post–dentin interface as a consequence of the use of high modulus materials [4,5]. Taking into account that stress concentration generally occurs at the apical and cervical regions of the tooth, flexible posts cause stress concentration in dentin, whereas rigid posts concentrate stresses at the interfaces [4,5].

Theoretical analyses have been employed to evaluate the influence of the shape, length, diameter, and stiffness of the post and the "ferrule effect" [9–11]. Specifically, an analysis of the stress distribution in endodontically treated canine teeth provided interesting results, demonstrating the synergistic contribution of the ferrule effect and the specific material–shape combination of the post [11].

In this context, dental posts with tailored properties have been developed using functionally graded materials in order to overcome all of the drawbacks related to the use of both rigid and flexible posts, and to optimize stress distribution [4,12]. Recently, a matrix of polyetherimide (PEI) reinforced with carbon (C) and glass (G) fibers was considered when designing a post with a Young's modulus varying from 57.7 to 9.0 GPa in the coronal-apical direction [13]. Finite element analysis of such a conceptual hybrid composite post demonstrated the most uniform stress distribution with no stress concentration in anterior teeth when compared to other C-G/PEI posts [13].

As a consequence, fiber-reinforced posts would seem to be the ideal solution as they possess Young's moduli which are lower than those of metal posts (e.g., 110 GPa for titanium and 95 GPa for gold) [5–8], also offering the possibility to tailor the modulus along the axial length [13].

The oral cavity is a unique environment and the continuous interaction with biological fluids may lead to the corrosion of metal materials, thus affecting their biocompatibility [14,15]. Even though it is documented that titanium (Ti) and nickel-chromium (Ni-Cr) alloy may cause allergic reactions [14,15], many theoretical and experimental studies have been performed on Ti and Ni-Cr posts [4,16–19]. In this context, materials with a Young's modulus similar to that of Ni-Cr alloy (200 GPa)—such as cobalt-chromium (Co-Cr) alloys (218 GPa)—have been further considered [19,20], and engineered ceramics such as yttria-partially stabilized zirconia (Y-TZP) (210 GPa) have been studied to design dental devices [20].

However, many post-core systems for endodontic treatment utilize a range of industrially developed posts, and posts with different materials, sizes, and shapes are usually considered for clinical use by endodontists [13].

Nevertheless, though it has been frequently reported that the great mismatch between the elastic modulus of metal posts and surrounding structures causes stress concentration and root fracture, it is also worth noting that stress distributions are related to stiffness, which depends upon the Young's modulus (an intrinsic mechanical property of the material), as well as shape and size.

Accordingly, the current research provides further insight into the effect of the material–shape combination of metal posts on the mechanical behavior of endodontically treated anterior teeth. In particular, the aim of this research was to analyze the stress distribution along the metal post and at the interface between the post and the surrounding structures, while varying the Young's modulus (the material) and shape (conical-tapered and conical-cylindrical). Materials with Young's moduli of 110 GPa and 200 GPa were considered for the analysis.

2. Materials and Methods

2.1. Post Design

Conceptual designs of metal posts with two different shapes (conical-tapered and conical-cylindrical) and consisting of materials with Young's moduli of 110 GPa and 200 GPa were proposed.

In particular, 15-mm-long metal posts with a conical-tapered shape (length of coronal-cylindrical part—7 mm; length of conicity part—8 mm; coronal diameters—Ø 1.05, Ø 1.25, and Ø 1.45; apical diameters—Ø 0.55, Ø 0.75, and Ø 0.95) and a conical-cylindrical shape (cylinder diameter—0.90 mm) were designed:

Post A1 (200 GPa, conical-tapered shape);
Post A2 (110 GPa, conical-tapered shape);
Post B1 (200 GPa, conical-cylindrical shape);
Post B2 (110 GPa, conical-cylindrical shape).

2.2. Solid Model Generation

An intact tooth (upper canine) was analyzed using a micro-CT scanner (Bruker micro-CT, Kontich, Belgium). Previously adopted methodologies were employed from the scanning through of the tessellated model [9,11,13,21,22]. As already specified [9,13], 252 slices were considered, although a total of 951 slices were collected at a resolution of 1024 × 1024 pixels [9,13]. In brief, ScanIP® (3.2, Simpleware Ltd., Exeter, UK) was used to process the image data sets. The three-dimensional (3D) tessellated model of the tooth was generated [9,11,13,21,22] as image segmentation and filtering procedures were properly employed [9,11,13,21,22]. Moreover, in order to convert tessellated models into surfaces, blending operations were performed through cross-sections according to the previously reported method [9,11]. The SolidWorks® 2017 (Dassault Systemes, Paris, France) computer-aided design (CAD) system was used to carry out such operations, and the ScanTo3D® add-in allowed for geometry management [9].

The length of the tooth was 25 mm, with a crown height of about 10 mm and a buccolingual crown diameter of about 7 mm [11,13,22]. With regard to crown preparation, tooth reduction was performed according to previous works (2.0 mm thickness of incisal edge, 1.0 mm thickness of facial edge, and 0.5 mm thickness of lingual edge) [11,13,22], where the model was properly located such that the *Z* axis was oriented apically, the *X* axis mesiodistally, and the *Y* axis buccolingually. Using the designed metal posts (A1, A2, B1, and B2), four different models of the restored tooth were created from the sound tooth model [11,13,22]. A cement layer of 0.1 mm in thickness was considered between the prepared crown and the abutment. The cement was added between the post and the root in the canal. In addition, the periodontal ligament was modeled as a 0.25-mm thin layer around the root.

2.3. Finite Element Analysis

The IGES format was used and the geometric models of the restored tooth were imported into HyperMesh® (HyperWorks®-14.0, Altair Engineering Inc., Troy, MI, USA), a typical finite element (FE) pre-processor which allows for the management and the generation of complex models, starting with the import of CAD geometry to export a ready-to-run solver file.

FE analysis was performed on the following models:

Model A1 (a tooth with Post A1);
Model A2 (a tooth with Post A2);
Model B1 (a tooth with Post B1);
Model B2 (a tooth with Post B2).

The model consisted of different components: A lithium disilicate crown; crown cement; an abutment; a post; post cement; a root; a periodontal ligament; and food (apple pulp) acting on the crown surface. The Young's modulus and Poisson's ratio for each component of the model are reported in Table 1.

Table 1. Mechanical properties of the model components: Young's modulus and Poisson's ratio [4,11,13].

Component	Young's Modulus (GPa)	Poisson's Ratio
Lithium disilicate crown	70	0.30
Crown cement	8.2	0.30
Abutment	12	0.30
Post A1 and Post B1	200	0.33
Post A2 and Post B2	110	0.35
Post cement	8.2	0.30
Root	18.6	0.31
Periodontal ligament	0.15 ($\times 10^{-3}$)	0.45
Food (apple pulp)	3.41 ($\times 10^{-3}$)	0.10

A 3D mesh was generated and 3D solid CTETRA elements with four grid points were considered for the models, according to a reported procedure [11,13]. Appropriate mesh size and refinement techniques were employed. Table 2 summarizes some technical features (total number of structural grids; elements excluding contact; node-to-node surface contact elements; and degrees of freedom) for the investigated models.

The analysis dealt with the closing phase of the chewing cycle and solid food (apple pulp [11]) acting on the crown surface (Figures 1 and 2). Slide-type contact elements were considered between the food and the tooth surface, whereas "freeze" type elements were used as the contact condition between different parts of the post restoration.

Table 2. Total number of grids (structural), elements excluding contact, node-to-node surface contact elements, and degrees of freedom.

Total # of Grids (Structural)	Total # of Elements Excluding Contact	Total # of Node-to-Node Surface Contact Elements	Total # of Degrees of Freedom
51,552	213,361	14,094	188,127

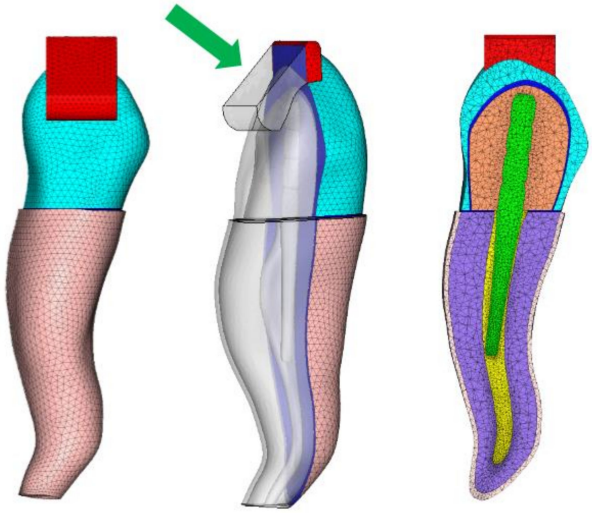


Figure 1. Models A1 and A2: Theoretical model according to the different components, mechanical properties, and technical and geometric features.

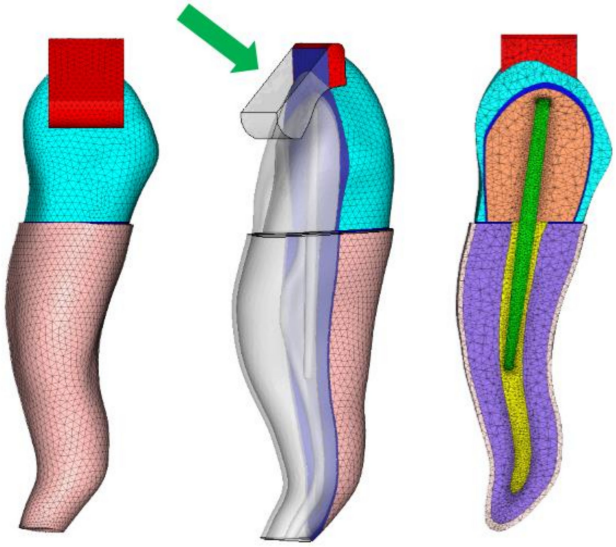


Figure 2. Models B1 and B2: Theoretical model according to the different components, mechanical properties, and technical and geometric features.

Concerning the external surfaces of the periodontal ligament, constraints were applied for nodal displacements in all of the directions [11,13]. A load of 100 N acted on the palatal surface of the crown and was applied at 45° to the longitudinal axis of the tooth.

Linear static analyses were carried out with a non-failure condition as all of the components were assumed to behave linearly elastic.

For all of the models, the maximum principal stress distribution was evaluated along the metal post as well as at the interface between the post and the surrounding structures in order to assess the effect of the post's material–shape combination.

3. Results and Discussion

Experimental methodologies and CAD-FE modeling have always played a crucial role in the analysis of the mechanical behavior, stress and strain distributions in different fields [11,23–27]. As widely reported, the use of a dental post with a high modulus material alters the biomechanical behavior of a restored tooth [4,12,13].

An ideal post should stabilize the core without weakening the root [4,12], and the stress transfer mechanism should avoid high stress concentrations [4,28,29] as a direct consequence of the stiffness mismatch between a post and surrounding structures [4,30].

Accordingly, over the past years great efforts have been made in the development of fiber-reinforced posts, as well as in the conceptual design of inhomogeneous dental posts [4], multilayer posts consisting of organic–inorganic hybrid materials [22], and C-G/PEI composite posts with a Young's modulus varying in the coronal-apical direction [13].

The conceptual solutions involved equations expressing the Young's modulus and Poisson's ratio as a function of the distance to the neutral axis of the post [4], as well as the CAD-based approach combined with the sol–gel chemical process [22], or with the possibility of tailoring the distance of carbon and glass fiber-reinforced plies from the middle plane in the coronal-apical direction [13].

In this context, even if stress concentration and root fracture are caused by the great mismatch between the elastic modulus of metal posts and the surrounding structures, it is also well known that the stress distribution is dependent on stiffness, which is related to the Young's modulus as well as shape and size.

For this reason, in the current study, conceptual designs of metal posts with two different shapes (conical-tapered and conical-cylindrical) and consisting of materials with Young's moduli of 110 GPa and 200 GPa were proposed and the effect on the mechanical behavior of endodontically

treated anterior teeth was analyzed, the aim being to provide further insight into the effect of the material–shape combination on metal posts.

The maximum principal stress distributions were evaluated in the abutment, post, post cement, root, and periodontal ligament (Figures 3 and 4), considering cross-sections along the buccolingual direction for all of the models.

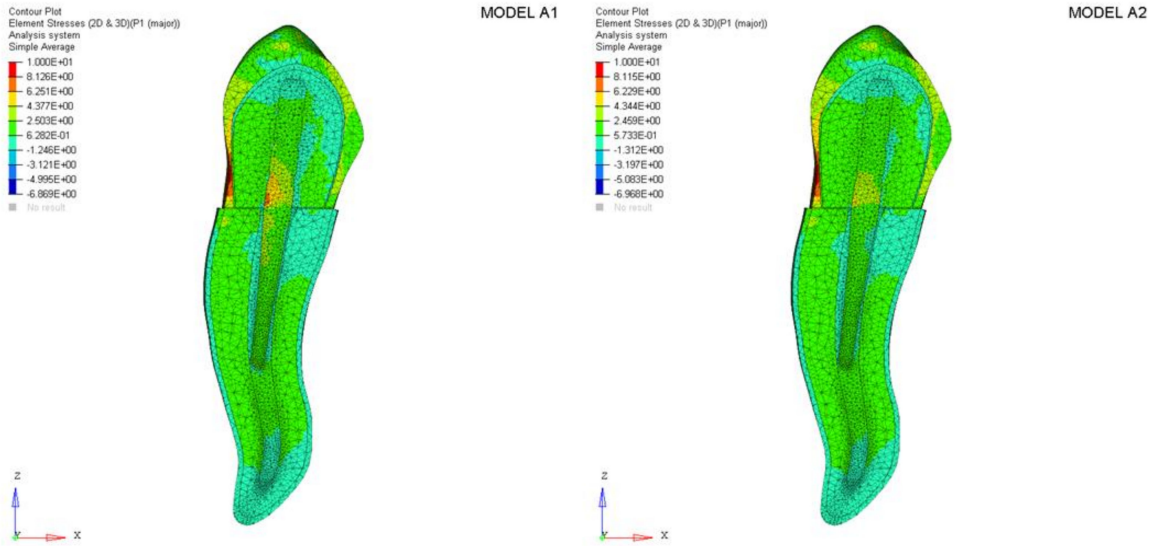


Figure 3. Models A1 and A2: Maximum principal stress distribution (MPa) in the post-restored tooth. The color scale was chosen to allow for comparison among the analyzed models.

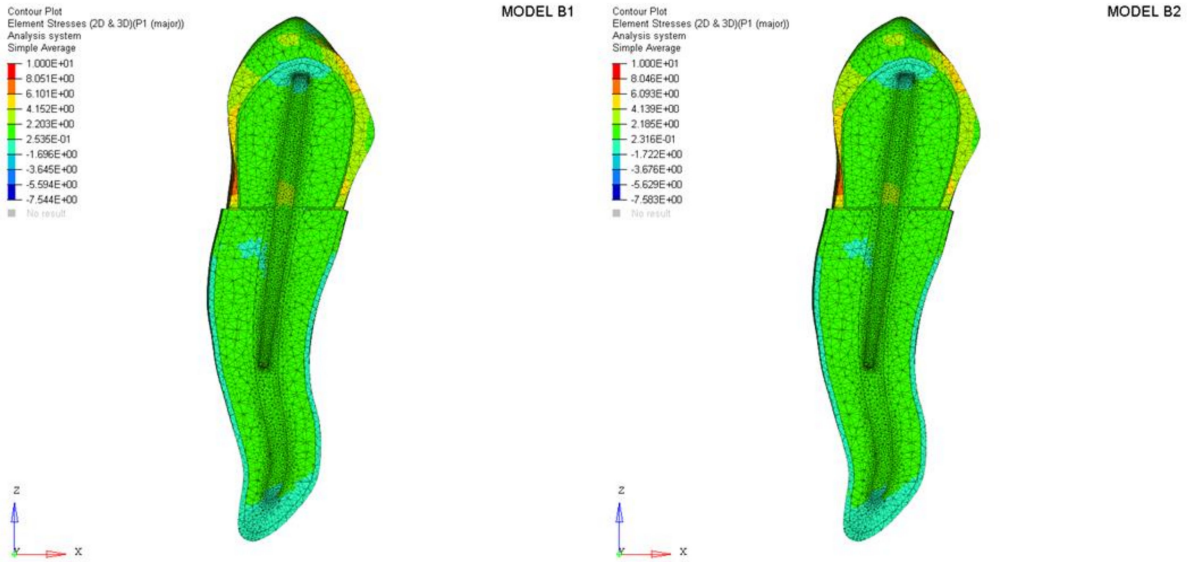


Figure 4. Models B1 and B2: Maximum principal stress distribution (MPa) in the post-restored tooth. The color scale was chosen to allow for comparison among the analyzed models.

The effect of the shape was evident since some differences were found in terms of stress distribution between models A1 and B1, as well as between models A2 and B2.

For each value of the modulus, higher stress regions were evident along the post near and under the cervical margin of the tooth in the case of conical-tapered shape when compared to those obtained for the conical-cylindrical shape.

However, the effect of the material was evident as a higher stress concentration was found for model A1 in comparison to model A2. Nevertheless, less marked differences were observed between

models B1 and B2, thus suggesting the effect of the material–shape combination on the mechanical behavior of endodontically treated anterior teeth.

The stress distribution along the post was also reported for all of the analyzed models (Figures 5–7).

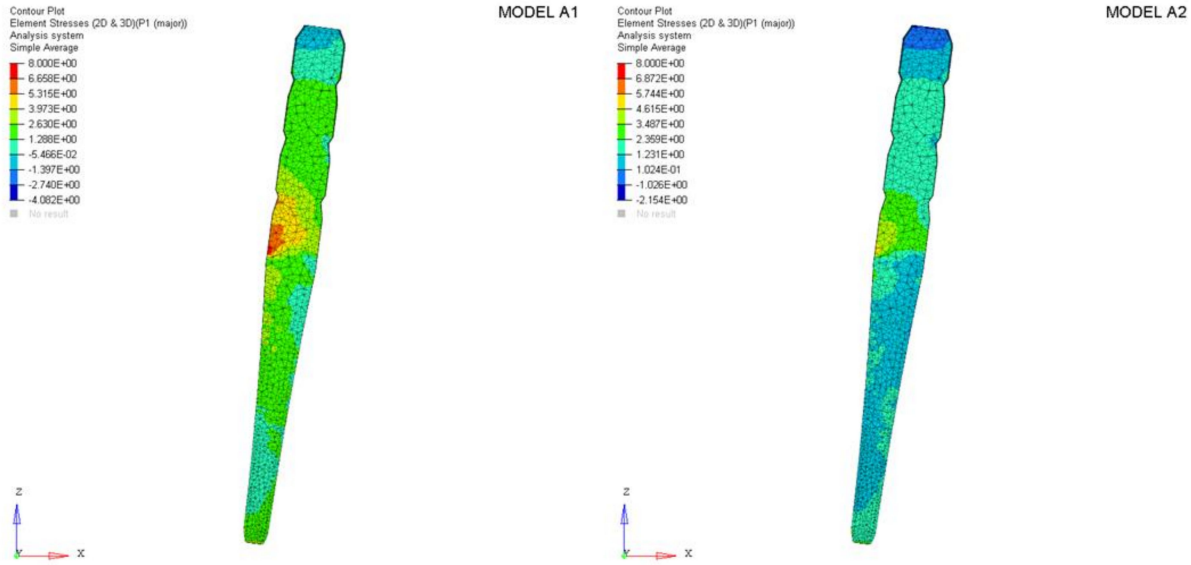


Figure 5. Models A1 and A2: Maximum principal stress distribution (MPa). The color scale was chosen to allow for comparison among the analyzed models.

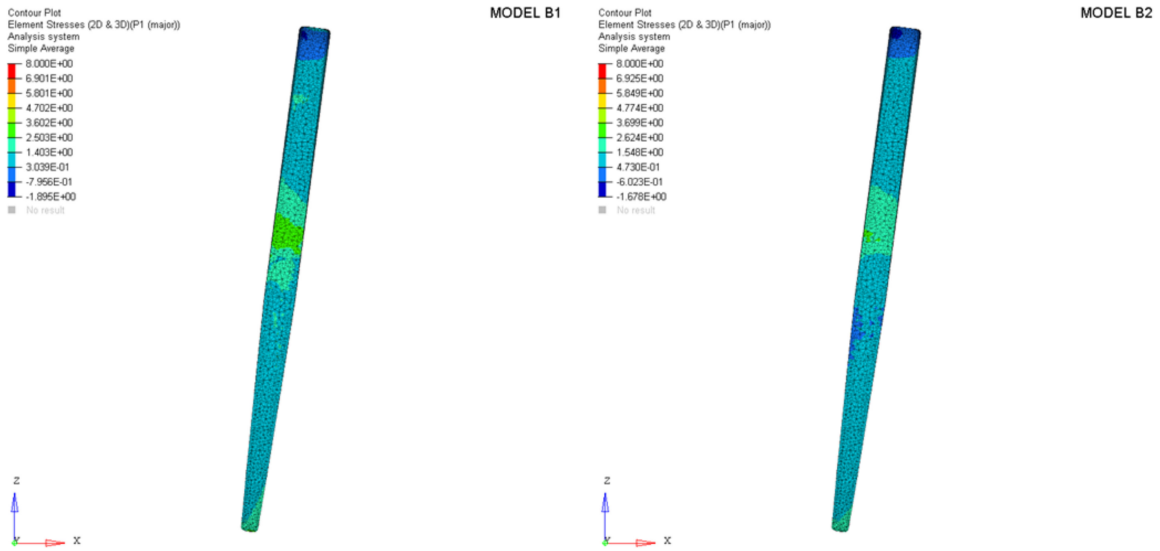


Figure 6. Models B1 and B2: Maximum principal stress distribution (MPa). The color scale was chosen to allow for comparison among the analyzed models.

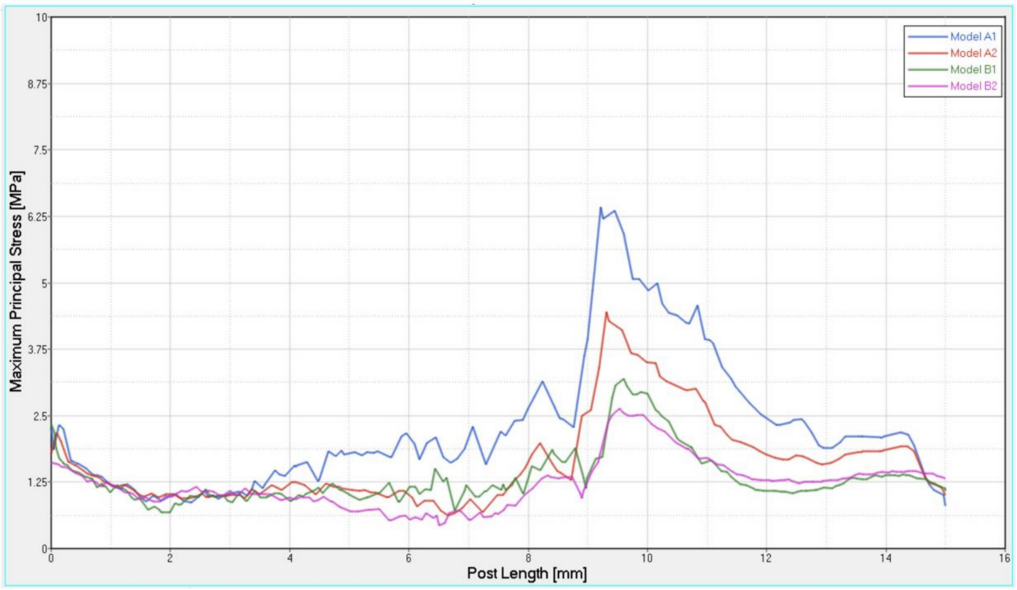


Figure 7. Models A1, A2, B1, and B2: Maximum principal stress distribution along the center of the post from the coronal to the apical part.

No great differences were observed for any of the models in the coronal region of the post, whereas higher values of maximum principal stress were observed along the post in models A1 and A2 when compared to models B1 and B2 (Figure 7). Similar values of maximum principal stress were achieved for models B1 and B2 (Figure 7). Thus, the results in terms of maximum principal stress distribution along the center of the post demonstrated the role of geometry and, in particular, the effect of the material–shape combination. Specifically, in comparison to post B1 (200 GPa, conical-cylindrical shape), higher stress values were obtained for post A2 (110 GPa, conical-tapered shape), even if the material of post A2 had a Young's modulus (110 GPa) [4] lower than that of the material of post B1 (200 GPa) [4] (Figure 7).

On the other hand, at the interface between the post and the surrounding structures, the analysis evidenced higher stress gradients for models A1 and B1 in comparison to models A2 and B2 (Figures 8–10).

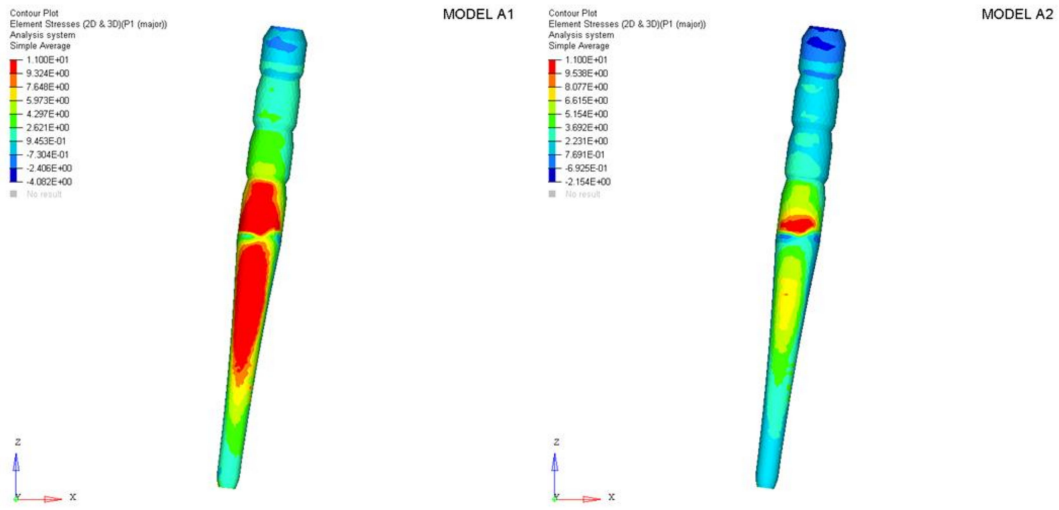


Figure 8. Models A1 and A2: Maximum principal stress distribution at the interface between the post and surrounding structures from the coronal to the apical part. The color scale was chosen to allow for comparison among the analyzed models.

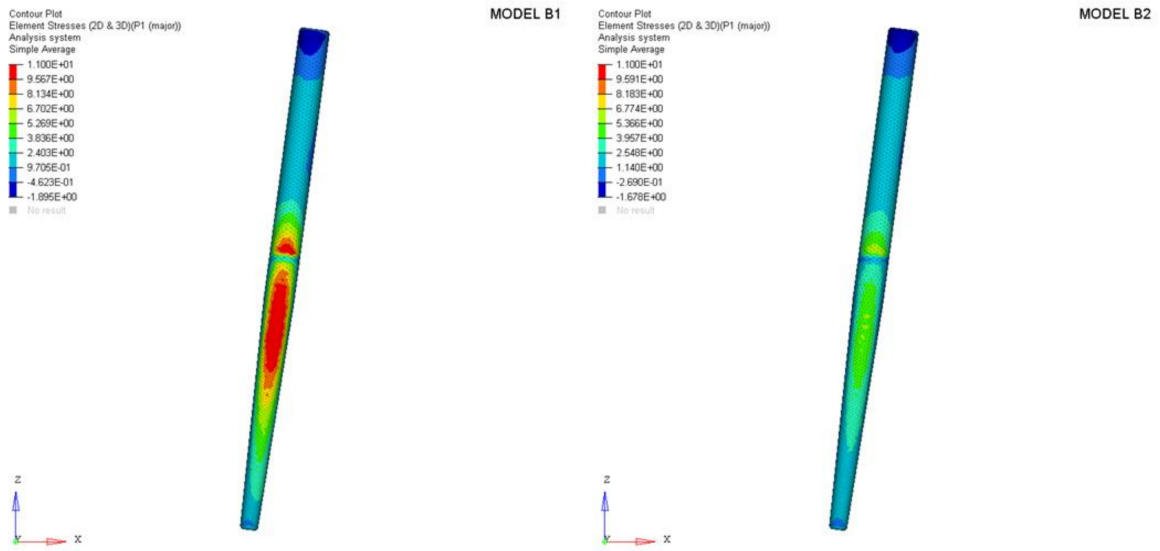


Figure 9. Models B1 and B2: Maximum principal stress distribution at the interface between the post and surrounding structures from the coronal to the apical part. The color scale was chosen to allow for comparison among the analyzed models.

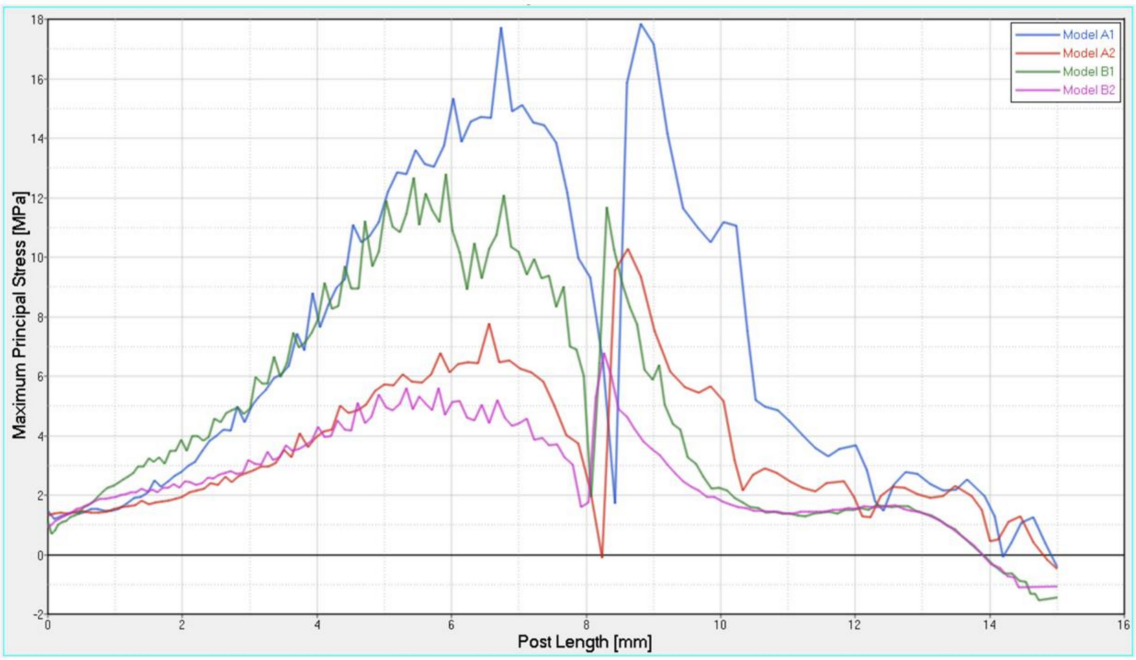


Figure 10. Models A1, A2, B1, and B2: Maximum principal stress distribution at the interface between the post and surrounding structures from the coronal to the apical part.

Differently from what was observed for the maximum stress distribution along the center of the post (Figure 7), with regard to the interface between the post and the surrounding structures (Figure 10), the higher the Young's modulus of the post, the higher the stress gradients—with some differences due to the specific geometry.

Furthermore, the lowest maximum principal stresses were found for post B2 (110 GPa, conical-cylindrical shape), whereas the greatest values were achieved for post A1 (200 GPa, conical-tapered shape).

Nevertheless, the obtained findings suggested a mostly uniform stress distribution with no significant stress concentration for post B2 (110 GPa, conical-cylindrical shape) in comparison to the other analyzed posts.

Although it has been frequently reported that fiber-reinforced posts associated with direct resin restorations can be seen as a faster therapeutic option for achieving good patient compliance [13,31,32], the present research also demonstrates the possibility to tailor the stress distributions in the case of metal posts, benefiting from the material–shape combination and, hence, from an appropriate combination of the CAD-based approach and material selection.

However, questions and contradictory opinions remain concerning clinical procedures, materials, and devices, even if much progress has been made in the field of endodontics, technologies, metallurgy, and materials science [29,32].

4. Conclusions

Despite the limitations of the current research, the following conclusions were reached:

1. FE analysis provided further insight into the effect of the material–shape combination of metal posts on the mechanical behavior of endodontically treated anterior teeth through varying material and shape.
2. The possibility to tailor the stiffness and, hence, the stress distribution through an appropriate material–shape combination was demonstrated for metal posts.
3. Post B2 (110 GPa, conical-cylindrical shape) provides better stress distribution as compared to the other analyzed posts.

Author Contributions: A.G. wrote the paper; A.G. and S.M. performed the FE analysis and analyzed the data; A.G., S.M., and M.M. provided information on the experimental/theoretical mechanical data; P.A. provided contributions and interpretations related to tooth structure, dental materials, clinical procedures, and endodontics; A.G. and M.R. performed the materials selection for post design according to the structure–property relationship; M.M, A.G., and M.R. performed the optimization of geometric features, CAD design, and solid model generation; A.G. and M.M. conceived of and designed the research.

Acknowledgments: The authors gratefully acknowledge Rodolfo Morra (Institute of Polymers, Composites, and Biomaterials, National Research Council of Italy) for providing information on methods for mechanical testing of dental materials and posts.

Conflicts of Interest: The authors declare no conflict of interest.

References

1. Zhu, M.; Xu, G.; Zhou, M.; Yuan, Q.; Tian, J.; Hu, H. Effects of Tempering on the Microstructure and Properties of a High-Strength Bainite Rail Steel with Good Toughness. *Metals* **2018**, *8*, 484. [CrossRef]
2. Fiorese, E.; Bonollo, F.; Battaglia, E. A Tool for Predicting the Effect of the Plunger Motion Profile on the Static Properties of Aluminium High Pressure Die Cast Components. *Metals* **2018**, *8*, 798. [CrossRef]
3. Jeon, G.T.; Kim, K.Y.; Moon, J.-H.; Lee, C.; Kim, W.-J.; Kim, S.J. Effect of Al 6061 Alloy Compositions on Mechanical Properties of the Automotive Steering Knuckle Made by Novel Casting Process. *Metals* **2018**, *8*, 857. [CrossRef]
4. Mahmoudi, M.; Saidi, A.R.; Amini, P.; Hashemipour, M.A. Influence of inhomogeneous dental posts on stress distribution in tooth root and interfaces: Three-dimensional finite element analysis. *J. Prosthet. Dent.* **2017**, *118*, 742–751. [CrossRef]
5. Lee, K.-S.; Shin, J.-H.; Kim, J.-E.; Kim, J.-H.; Lee, W.-C.; Shin, S.-W.; Lee, J.-Y. Biomechanical evaluation of a tooth restored with high performance polymer PEKK post-core system: A 3D finite element analysis. *Biomed. Res. Int.* **2017**, *2*, 1–9.
6. Cheleux, N.; Sharrock, P.J. Mechanical properties of glass fiber-reinforced endodontic posts. *Acta Biomater.* **2009**, *5*, 3224–3230. [CrossRef] [PubMed]
7. Sakaguchi, R.L.; Powers, J.M. *Craig's Restorative Dental Materials-e-book*; Elsevier Health Sciences: New York, NY, USA, 2018.
8. Craig, R.; Peyton, F. Elastic and mechanical properties of human dentin. *J. Dent. Res.* **1958**, *37*, 710–718. [CrossRef] [PubMed]
9. Ausiello, P.; Franciosa, P.; Martorelli, M.; Watts, D.C. Mechanical behavior of post-restored upper canine teeth: A 3D FE analysis. *Dent. Mater.* **2011**, *27*, 285–1294. [CrossRef] [PubMed]

10. Dejak, B.; Młotkowski, A. The influence of ferrule effect and length of cast and FRC posts on the stresses in anterior teeth. *Dent. Mater.* **2013**, *29*, e227–e237. [CrossRef]
11. Ausiello, P.; Ciaramella, S.; Martorelli, M.; Lanzotti, A.; Zarone, F.; Watts, D.C.; Gloria, A. Mechanical behavior of endodontically restored canine teeth: Effects of ferrule, post material and shape. *Dent. Mater.* **2017**, *33*, 1466–1472. [CrossRef]
12. Abu Kasim, N.H.; Madfa, A.A.; Hamdi, M.; Rahbari, G.R. 3D-FE analysis of functionally graded structured dental posts. *Dent. Mater.* **2011**, *30*, 869–880. [CrossRef] [PubMed]
13. Gloria, A.; Maietta, S.; Martorelli, M.; Lanzotti, A.; Watts, D.C.; Ausiello, P. FE analysis of conceptual hybrid composite endodontic post designs in anterior teeth. *Dent. Mater.* **2018**, *34*, 1063–1071. [CrossRef]
14. Chaturvedi, T.P. Allergy related to dental implant and its clinical significance. *Clin. Cosmet. Investig. Dent.* **2013**, *5*, 57–61. [CrossRef] [PubMed]
15. Meena, S.; Radhika, C.; Vinod, S. Allergic Reactions to Dental Materials-A Systematic Review. *J. Clin. Diagn. Res.* **2015**, *9*, ZE04–ZE09.
16. Kadhim, K.R. Study of Using the Ni-Cr Alloy Post and Increasing Cement Strength (Zinc Polycarboxylate) on the Stress Distribution of Restored Human Tooth. *J. Eng. Dev.* **2011**, *15*, 1813–7822.
17. Borhan Haghighi, Z.; Pahlavanpour Fard Jahromy, A.M. Comparison of Fracture Strength of Endodontically Treated Teeth Restored with Two Different Cast Metallic Post Systems. *J. Dent. Biomater.* **2014**, *1*, 45–49.
18. Madfa, A.A.; Al-Hamzi, M.A.; Al-Sanabani, F.A.; Al-Qudaim, N.H.; Guang, Y.X. 3D FEA of cemented glass fiber and cast posts with various dental cements in a maxillary central incisor. *Springerplus* **2015**, *4*, 598. [CrossRef] [PubMed]
19. Eakle, W.S.; Hatrick, C. *Dental Materials—Clinical Applications for Dental Assistants and Dental Hygienists*, 3rd ed.; Elsevier: St. Louis, MO, USA, 2016.
20. Pérez-Pevida, E.; Brizuela-Velasco, A.; Chávarri-Prado, D.; Jiménez-Garrudo, A.; Sánchez-Lasheras, F.; Solaberrieta-Méndez, E.; Diéguez-Pereira, M.; Fernández-González, F.J.; Dehesa-Ibarra, B.; Monticelli, F. Biomechanical Consequences of the Elastic Properties of Dental Implant Alloys on the Supporting Bone: Finite Element Analysis. *Biomed Res. Int.* **2016**, 1850401. [CrossRef] [PubMed]
21. Rodrigues, F.P.; Li, J.; Silikas, N.; Ballester, R.Y.; Watts, D.C. Sequential software processing of micro-XCT dental-images for 3D-FE analysis. *Dent. Mater.* **2009**, *25*, 47–55. [CrossRef]
22. Maietta, S.; De Santis, R.; Catauro, M.; Martorelli, M.; Gloria, A. Theoretical Design of Multilayer Dental Posts Using CAD-Based Approach and Sol-Gel Chemistry. *Materials* **2018**, *11*, 738. [CrossRef]
23. Ausiello, P.; Ciaramella, S.; Garcia-Godoy, F.; Martorelli, M.; Sorrentino, R.; Gloria, A. Stress distribution of bulk-fill resin composite in class II restorations. *Am. J. Dent.* **2017**, *30*, 227–232. [PubMed]
24. Ausiello, P.; Ciaramella, S.; Martorelli, M.; Lanzotti, A.; Gloria, A.; Watts, D.C. CAD-FE modeling and analysis of class II restorations incorporating resin-composite, glass ionomer and glass ceramic materials. *Dent. Mater.* **2017**, *33*, 1456–1465. [CrossRef] [PubMed]
25. Maietta, S.; Russo, T.; De Santis, R.; Ronca, D.; Riccardi, F.; Catauro, M.; Martorelli, M.; Gloria, A. Further Theoretical Insight into the Mechanical Properties of Polycaprolactone Loaded with Organic–Inorganic Hybrid Fillers. *Materials* **2018**, *11*, 312. [CrossRef]
26. Martorelli, M.; Maietta, S.; Gloria, A.; De Santis, R.; Pei, E.; Lanzotti, A. Design and analysis of 3D customized models of a human mandible. *Procedia CIRP* **2016**, *49*, 199–202. [CrossRef]
27. Caputo, F.; De Luca, A.; Greco, A.; Maietta, S.; Marro, A.; Apicella, A. Investigation on the static and dynamic structural behaviours of a regional aircraft main landing gear by a new numerical methodology. *Frattura Integr. Strutt.* **2018**, *12*, 191–204.
28. Grandini, S.; Sapio, S.; Simonetti, M. Use of anatomic post and core for reconstructing an endodontically treated tooth: A case report. *J. Adhes. Dent.* **2003**, *5*, 243–247. [PubMed]
29. Wilson, P.D.; Wilson, N.; Dunne, S. *Manual of Clinical Procedures in Dentistry*; John Wiley & Sons: Hoboken, NJ, USA, 2018.
30. Manhart, J. Fiberglass reinforced composite endodontic posts. *Endodontic Pract.* **2009**, *September*, 16–20.

31. Grandini, S.; Goracci, C.; Tay, F.R.; Grandini, R.; Ferrari, M. Clinical evaluation of the use of fiber posts and direct resin restorations for endodontically treated teeth. *Int. J. Prosthodont.* **2005**, *18*, 399–404. [PubMed]
32. Faria, A.C.; Rodrigues, R.C.; de Almeida Antunes, R.P.; de Mattos Mda, G.; Ribeiro, R.F. Endodontically treated teeth: Characteristics and considerations to restore them. *J. Prosthodont. Res.* **2011**, *55*, 69–74. [CrossRef]



© 2019 by the authors. Licensee MDPI, Basel, Switzerland. This article is an open access article distributed under the terms and conditions of the Creative Commons Attribution (CC BY) license (http://creativecommons.org/licenses/by/4.0/).